Cagelike Precursors of High-Molar-Mass Silsesquioxanes Formed by the Hydrolytic Condensation of Trialkoxysilanes

Patricia Eisenberg,[†] Rosa Erra-Balsells,[*,§] Yoko Ishikawa,[⊥] Juan C. Lucas,[†] Adriana N. Mauri,[‡] Hiroshi Nonami,[⊥] Carmen C. Riccardi,[‡] and Roberto J. J. Williams[*,‡]

Institute of Materials Science and Technology (INTEMA), University of Mar del Plata-CONICET, J. B. Justo 4302, 7600 Mar del Plata, Argentina; Department of Organic Chemistry, University of Buenos Aires, Pab. 2, Ciudad Universitaria, 1428 Buenos Aires, Argentina; Technological Research Center for the Plastics Industry (CITIP, INTI), INDEMAT (University of San Martín), C.C. 157, 1650 San Martín, Argentina; and Plant Biophysics/Biochemistry Research Laboratory, College of Agriculture, Ehime University, Matsuyama 790-8566, Japan

Received July 27, 1999; Revised Manuscript Received December 14, 1999

ABSTRACT: High-molar-mass silsesquioxanes (SSQO) based on (3-glycidoxypropyl)trimethoxysilane (GPMS) and (3-methacryloxypropyl)trimethoxysilane (MPMS) were synthesized. The hydrolytic condensation of GPMS was performed using HCOOH (0.1 N) as catalyst, keeping the molar ratio $H_2O/Si = 3$. A first step was performed in tetrahydrofuran (THF) at 50 °C, followed by a second step in diglycidyl ether of bisphenol A (DGEBA), where temperature was increased in steps up to 140 °C. The hydrolytic condensation of MPMS was performed in bulk with HCOOH 98%, at $T = 50$ or 70 °C, using molar ratios of HCOOH/Si = 3 or 6. Homogeneous solutions were obtained for both silanes. The reaction was followed by size exclusion chromatography (SEC), and final products were characterized by matrix-assisted ultraviolet laser desorption/ionization time-of-flight mass spectrometry (UV-MALDI-TOF MS), FTIR, and ^{1}H and ^{29}Si NMR. Molar-mass distributions showed the presence of clusters corresponding to products formed in different generations. With the aid of UV-MALDI-TOF MS, the different species present in every cluster could be identified for one of the silsesquioxanes derived from MPMS. During the initial stage of the hydrolytic condensation, species with 7−12 Si atoms were produced. They mainly consisted of incompletely condensed polyhedra (species with 1−3 OH per molecule) and ladder-type structures (species with 4 OH per molecule). Species with more OH groups were condensed with a higher probability, giving place to a second generation of products. This process accounts for the presence of a cluster of species with 14−24 Si atoms and the enrichment of the first cluster in the more condensed structures ($T_7(OH)$, $T_8(OH)_2$, and $T_9(OH)$). Third and fourth generations of condensation products were also present. Structures of different species may be depicted as combinations of incompletely condensed polyhedra with ladder fragments.

Introduction

Silsesquioxanes (SSQO) are the generic products obtained by the hydrolytic condensation of monomers such as trichloro- or trialkoxysilanes or the condensation of trihydroxysilanes. Strictly speaking, the term refers to fully condensed structures of formula $(RSiO_{1.5})_n$ (n = even number), also denoted as T_n or as polyhedral oligosilsesquioxanes (POSS). But the term is frequently extended to denote partially condensed structures: $[RSiO_{1.5-x}(OH)_{2x}]_n$ or $T_n(OH)_m$, where $m = 0, 2, 4, ..., (2 + n)$ for n = even number and $m = 1, 3, 5, ..., (2 + n)$ for n = odd number. Keeping this extended definition, SSQO structures may vary from perfect polyhedra, incompletely condensed polyhedra, ladder polymers, open structures, linear polymers, and all their possible combinations. Figure 1 shows some possible structures for an octasilsesquioxane.

An extensive experimental work on the isolation and characterization of intermediates produced during the synthesis of several silsesquioxanes was carried out by Brown et al. in the 1960s.[1−3] Although the first oligomers generated in the polymerization could be identified, the structure of larger species was assigned in a rather speculative way, so that the mechanism of the polymer growth could not be ascertained. For example, the hydrolytic condensation of cyclohexyltrichlorosilane in aqueous acetone led to the dimer, trimer, and tetramer that were easily isolated. Further condensation gave a resinous mixture which very slowly converted to two crystalline species: T_6 and $T_7(OH)_3$, which were continuously precipitated from the reaction mixture.[2] Feher et al.[4] reanalyzed this synthesis and showed that a $T_8(OH)_2$ species also precipitated with the two other oligomers. The combined yield of the three products from a typical reaction was 60−70%. Larger species formed part of a "resinous liquid" that was not characterized. The hydrolytic condensation of phenyltrichlorosilane in aqueous acetone led to $T_4(OH)_4$ and $T_8(OH)_2$ isomers as well as other 8−12-unit cagelike polyhedra. In less polar solvents, the size of the larger species increased from 8 to 12 to 20−30 units.[3]

The selected examples give evidence of the presence of an unusual polymerization mechanism, generating cyclic and cagelike products during the first stages of the hydrolytic condensation. However, later stages have not been studied in detail. Brown[3] suggested that the structure of high-molar-mass silsesquioxanes should resemble irregularly branched strings of beads (the "beads" being the cagelike intermediates formed in the

* Authors for correspondence. E-mails: williams@fi.mdp.edu.ar; erra@qo.fcen.uba.ar.
‡ INTEMA.
† CITIP (INTI) and INDEMAT.
§ University of Buenos Aires.
⊥ Ehime University.

10.1021/ma9912507 CCC: $19.00
Published on Web 03/01/2000

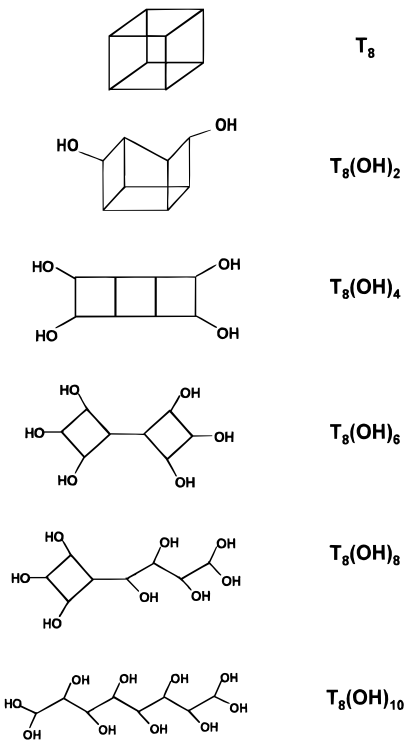

Figure 1. Examples of some possible structures for the octasilsesquioxane: $T_8(OH)_m$ (segments represent Si−O−Si bonds; the organic group R is attached to every Si atom).

first stage). But other different structures are frequently proposed such as randomly connected three-dimensional networks of trifunctional monomers, "ladder" structures, and a combination of linear, "ladder", and cagelike fragments.[5,6]

Piana and Schubert[7] studied the catalyst influence on the molar mass distribution of hydrolyzed (3-glycidoxypropyl)trimethoxysilane (GPMS) and (3-methacryloxypropyl)trimethoxysilane (MPMS). The development of molar-mass distributions was followed by size exclusion chromatography (SEC). In the presence of 1-methylimidazol as catalyst, GPMS led to clusters of oligomers centered at about $n = 8$ and 16, based on polystyrene standards. For MPMS, the molar-mass distributions depended on the type of catalyst used, but the appearance of the chromatograms showed the presence of a polymodal distribution of oligomeric species.

The molar-mass distribution of silsesquioxanes may be conveniently determined using matrix-assisted ultraviolet laser desorption/ionization time-of-flight mass spectrometry (UV-MALDI-TOF MS). This technique was recently applied to analyze the distribution of oligomeric species in a silsesquioxane obtained by the hydrolytic condensation of MPMS.[8] Oligomers were detected from m/z about 1100 ($n = 6$) to about 12 000 (n close to 65), the lower limit being defined by matrix interference and the upper limit by the signal-to-noise ratio. Every value of n was represented in the distribution. No fully condensed polyhedra were observed except at very low mass ($n < 10$). The average number of OH groups in the generic $T_n(OH)_m$ structure was $m = 2 + 0.454n$. For example, for $n = 8$ this gives $m = 5.632$, meaning that relatively open structures (close to the structure of $T_8(OH)_6$, shown in Figure 1) are formed under the particular experimental conditions used to synthesize this SSQO.[9]

To analyze in more detail the formation mechanism of high-molar-mass silsesquioxanes, we performed the hydrolytic condensation of GPMS and MPMS in conditions that avoided both the formation of precipitates and the overall gelation. SEC results provided direct evidence of the presence of a cluster-growth mechanism. FTIR, ^{1}H NMR, and ^{29}Si NMR were used to characterize the structures of the condensation products, and UV-MALDI-TOF MS was used to determine the molar-mass distribution of the SSQO based on MPMS. A possible mechanism of the polymer growth is discussed.

Experimental Section

Materials. Chemical structures of the trialkoxysilanes and the epoxy solvent are shown in Figure 2. Both silanes—(3-glycidoxypropyl)trimethoxysilane (GPMS, Sigma) and (3-methacryloxypropyl)trimethoxysilane (MPMS, Dow Corning Z-6030)—were used as received. The solvent selected for the final step of the hydrolytic condensation of GPMS was diglycidyl ether of bisphenol A (DGEBA, MY 790 Ciba, with an average n value equal to 0.03).

Hydrolytic Condensation. The hydrolytic condensation of GPMS was performed in three steps. The first one was carried out using tetrahydrofuran (THF) as solvent, at a concentration of 1.5 g/mL, and HCOOH (0.1 N) as catalyst, keeping the molar ratio $H_2O/Si = 3$. The reaction was carried out for 24 h at 50 °C. The second step was performed by adding DGEBA as solvent, in an amount such that 50% of the epoxy groups were contributed by the silsesquioxane. The hydrolytic condensation was performed for another 24 h at 70 °C (THF was removed in this step). The third and final step was performed using the following heating schedule: 3 h at 75 °C, 6 h at 105 °C, and 6 h at 140 °C. The solution remained homogeneous during the three steps.

The hydrolytic condensation of MPMS was performed in bulk, using HCOOH 98% in a molar ratio HCOOH/Si = 3 or 6, at $T = 50$ or 70 °C, for several days. The mechanism by which concentrated formic acid produces the condensation of alkoxysilanes has been described in the literature.[10]

Characterization. The molar-mass distribution was followed by size exclusion chromatography (SEC, Shimadzu GPC 80), using columns 801, 802, and 803 covering the range of molar masses comprised between 10^2 and 10^5, a refractive index detector, THF at 1 mL/min as carrier, and butylated hydroxytoluene, BHT, as internal standard. When using DGEBA as solvent, the elution time of the isomer with $n = 0$ (Figure 2) was close to the one of BHT. So, retention times of different products were referred to BHT through the DGEBA isomer with $n = 1$ (Figure 2). Retention times of polystyrene (PS) standards were also determined.

^{1}H NMR spectra were recorded with a Bruker AC200 spectrometer operating at 200.133 MHz. ^{29}Si NMR spectra were recorded with a Bruker AM500 spectrometer operating at 99.364 MHz. Samples were dissolved in deuterated acetone except for the ^{1}H NMR characterization of the SSQO derived from MPMS, which was performed in deuterated chloroform. Chemical shifts are reported as δ units (ppm) relative to tetramethylsilane. Residual solvent peaks were used as internal standards for ^{1}H NMR, and hexamethyldisiloxane (HMDS) was used as external standard for ^{29}Si chemical shifts. The digital resolution for ^{29}Si proton decoupled spectra was 0.636 Hz.

FTIR spectra were recorded either with a Bruker IFS 25 or a Nicolet-Omnic 500, in the transmission mode. Silsesquioxanes were coated on NaCl windows from acetone solutions.

Matrix-Assisted Ultraviolet Laser Desorption/Ionization Time-of-Flight Mass Spectrometry (UV-MALDI-TOF MS). Several chemicals were attempted as matrices: β-carbolines[11,12] (9*H*-Pyrido[3,4-*b*]indole (nor-harmane), 1-methyl-9*H*-pyrido[3,4-*b*]indole (harmane), 7-methoxy-1-methyl-9*H*-pyrido[3,4-b]indole (harmine), 7-methoxy-1-methyl-3,4-dihydro-9*H*-pyrido[3,4-b]indole (harmaline)), and classical matrices[13] (2,5-dihydroxybenzoic acid (gentisic acid, GA); 3,5-dimethoxy-

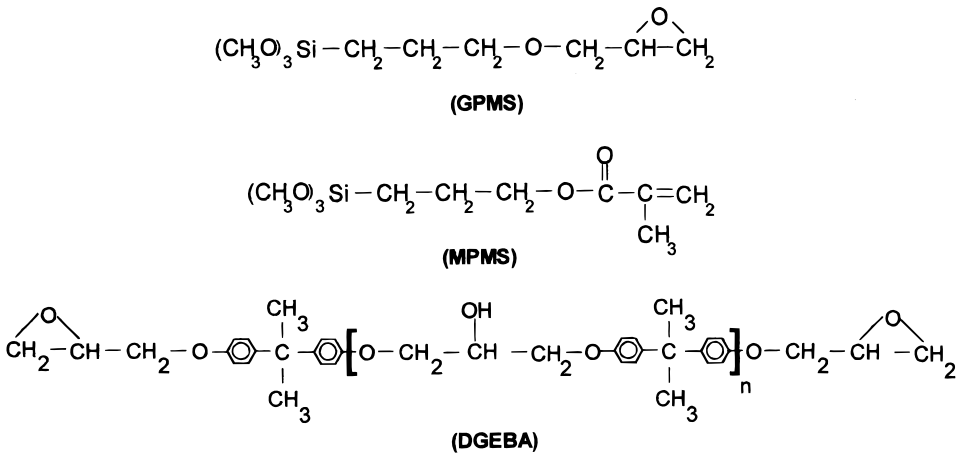

Figure 2. Chemical structures of silanes and the epoxy solvent.

4-hydroxycinnamic acid (SA); 1,8-dihydroxy-9(10*H*)anthracenone (dithranol), *trans*-3-indoleacrylic acid (IAA), 7-amino-2-hydroxy-4-methylquinoline (carbostyril 124), and 2-(4-hydroxyphenylazo)-benzoic acid (HABA)). These chemicals were purchased from Sigma, Aldrich, Acros Organics (Japan), and Wako Pure Chemical Ind. (Japan). The best results were obtained by using nor-harmane, GA, and IAA.

Several proteins (Sigma) dissolved in aqueous 0.1% TFA (Merck) and cyclodextrins (Sigma) in water (Milli-Q grade) solution were used for calibration purposes. Solutions of the matrix and the silsesquioxane (analyte) were performed in THF (Aldrich, HPLC grade). To study the effect of Ag and Na ions on the MALDI spectra, 4.5×10^{-3} M solutions of silver trifluoroacetate (AgTFA) and silver acetylacetonate (Ag(acac)) in THF and NaCl in water were used.

Two methods of sample preparation were used. In method A, 0.5 μL of the matrix solution was placed on the sample probe tip, and the solvent was removed by blowing air at room temperature. Then, 0.5 μL of the analyte solution was placed and the solvent removed. This was followed by two additional coatings with the matrix solution. In method B, matrix and analyte solutions were mixed in different volumetric ratios, and two coatings (0.5 μL each) were performed. When doping with Ag^+ in method A, 0.5 μL of the corresponding solution was added following the analyte. When doping with Ag^+ or Na^+ in method B, coating of the probe tip with the corresponding solution was the first step, followed by the usual procedure.

Measurements were performed using (i) a Shimadzu Kratos, Kompact MALDI III UV-laser desorption time-of-flight mass spectrometer and (ii) a Shimadzu Kratos, Kompact MALDI 4 (pulsed extraction, with tunable time delay capability). Both spectrometers are equipped with a pulsed nitrogen laser (λ = 337 nm; pulse width = 3 ns). TOF analyzers were used at 20 kV, and ions were obtained by irradiation just above the threshold laser power. Samples were measured in the linear mode, in both positive and negative ion modes. Usually 50 spectra were accumulated.

Results and Discussion

SEC Chromatograms in the Course of the Hydrolytic Condensation. Figure 3 shows SEC chromatograms of the products obtained after the different steps of the hydrolytic condensation. Peaks in Figure 3a are assigned to the internal standard (BHT) and the hydrolyzed monomer, $T(OH)_3$; dimer, $T_2(OH)_4$; trimers, $T_3(OH)_5$ or $T_3(OH)_3$; and tetramer, $T_4(OH)_4$. The presence of similar products was reported during the first stages of the uncatalyzed hydrolytic condensation of GPMS.[7] Relative retention times with respect to BHT are plotted in Figure 4 as a function of the molar mass. Experimental values of two low-molar-mass PS standards are also plotted.

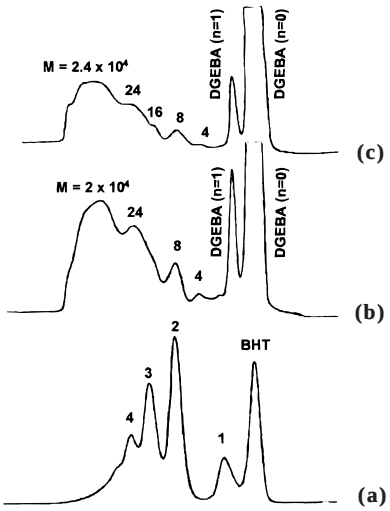

Figure 3. SEC chromatograms of the products obtained by the hydrolytic condensation of GPMS. (a) After the first step: 24 h at 50 °C in THF. (b) After the second step: 24 h at 70 °C in DGEBA. (c) After the third step: heating with a thermal cycle attaining 140 °C. An expanded scale of elution volumes was used for curve a.

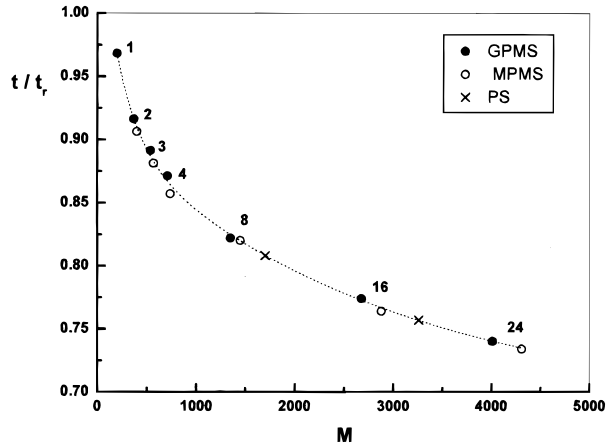

Figure 4. Relative retention times with respect to the internal standard (BHT), for products obtained by the hydrolytic condensation of GPMS and MPMS, and for polystyrene standards (PS), as a function of the molar mass, in the 100–4500 range. (The number of Si atoms in the different products is indicated.)

The peak that appears next to the tetramer in Figure 3b is assigned to a cluster of species centered at about $n = 8$: $T_8(OH)_m$,based on PS standards. (The point is

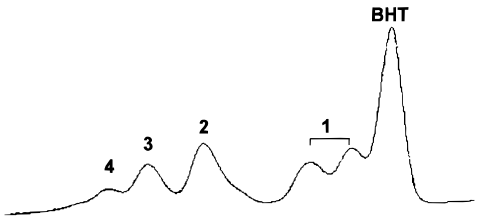

Figure 5. SEC chromatogram of the reaction products obtained after 15 min of hydrolytic condensation of MPMS at 50 °C (HCOOH/Si = 3).

arbitrarily represented using $m = 2$ in Figure 4.) The next peak in Figure 3b is assigned to a cluster of species centered at about $n = 24$, $T_{24}(OH)_m$ (again, $m = 2$ was arbitrarily used), and the high-molar-mass peak corresponds to an average mass close to 2×10^4, both based on PS standards. The third step of the hydrolytic condensation shows an increase of the average molar mass as well as the presence of a small shoulder corresponding to a cluster of species centered at about $n = 16$ (also located in Figure 4, taking $m = 2$).

SEC chromatograms give evidence of the presence of a polymodal distribution with species assembled in clusters. If the cluster centered at about $n = 8$ is regarded as a fundamental building block, next clusters exhibit an average mass that is 2 and 3 times its mass. Then, it may be inferred that the SSQO structure is built up by a cluster-growth mechanism.

For the case of MPMS, the absence of solvent and the use of concentrated formic acid made the hydrolytic concentration proceed at a fast rate since time zero. Figure 5 shows a SEC chromatogram obtained after 15 min reaction (HCOOH/Si = 3, $T = 50$ °C). Two different monomers (with different degrees of hydrolysis) were present, together with peaks assigned to the dimer, $T_2(OH)_4$; trimers, $T_3(OH)_5$ and $T_3(OH)_3$; and tetramer, $T_4(OH)_4$. These species are also included in the calibration curve of Figure 4.

The evolution of SEC chromatograms with reaction time is shown in Figure 6. The peak appearing next to the tetramer is assigned to a cluster centered at about $n = 8$: $T_8(OH)_m$,based on PS standards. The next peak present at 41 h and longer periods has an average mass that is about twice the mass of the first cluster, on the basis of PS standards. It is then assigned to a cluster centered at n close to 16: $T_{16}(OH)_m$. After prolonged storage periods at room temperature, a small increase in the peak of $n = 16$ was observed at the expense of a small decrease of the peak of $n = 8$. Although this trend continued after several months of storage at room temperature, the stability of the synthesized silsesquioxane with respect to gelation or precipitation was excellent. This is an important aspect to consider for application purposes.

To force the generation of high-molar-mass oligomers, the hydrolytic condensation was performed at 70 °C, keeping the molar ratio HCOOH/Si = 3. Figure 7 shows the molar-mass distribution after 8 days. The high-molar-mass peak shows a mass that is about 3 times the mass of the first cluster, on the basis of PS standards. It was then assigned to the cluster centered at about $n = 24$: $T_{24}(OH)_m$.

Still larger molar masses were obtained by keeping $T = 70$ °C but using a ratio HCOOH/Si = 6. The SEC chromatogram obtained after 8 days of hydrolytic condensation (Figure 8) showed small concentrations of

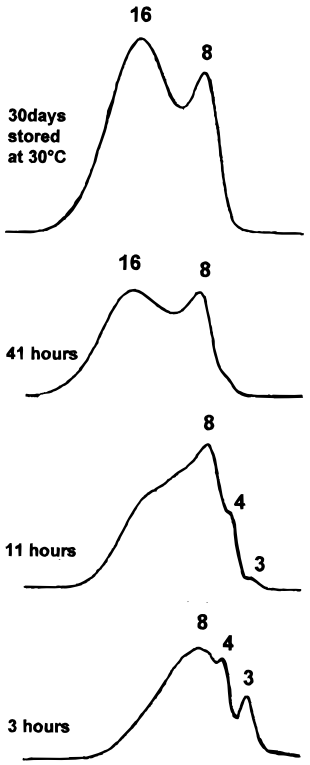

Figure 6. Evolution of SEC chromatograms during the hydrolytic condensation of MPMS at 50 °C (HCOOH/Si = 3).

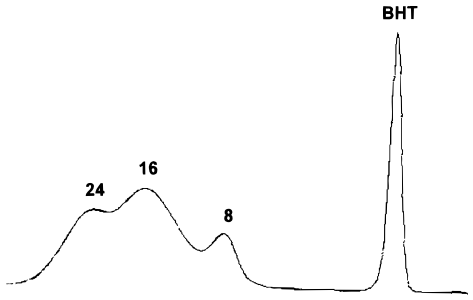

Figure 7. SEC chromatogram after 8 days of hydrolytic condensation of MPMS at 70 °C (HCOOH/Si = 3).

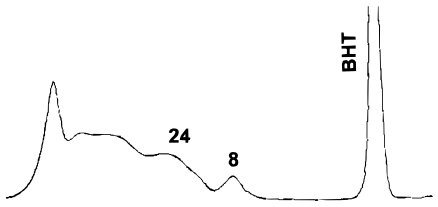

Figure 8. SEC chromatogram after 8 days of hydrolytic condensation of MPMS at 70 °C (HCOOH/Si = 6).

the first and third cluster together with a large concentration of high-molar-mass species.

Then, SEC chromatograms obtained during the hydrolytic condensation of GPMS and MPMS show that a cluster-growth mechanism is operative under the selected experimental conditions. During the first stages of the reaction, clusters of species containing about eight Si atoms are generated. Next clusters exhibit average masses that are approximately 2 and 3 times the average mass of the first cluster (based on PS standards; $m = 2$ was taken to represent the points in Figure 4). Clusters of larger molar masses are slowly generated at the expense of those of lower molar masses.

To get more information on the structure of both silsesquioxanes, ^{1}H NMR, ^{29}Si NMR, and FTIR spectra were analyzed.

^{1}H NMR, ^{29}Si NMR, and FTIR Characterization of the SSQO Based on GPMS. ^{1}H NMR spectra showed that the epoxy rings of both GPMS and DGEBA were not reacted even after the thermal treatment to 140 °C. This was proved by the constancy of the ratio of the number of protons of the epoxy ring in DGEBA (2.68, 2.79, and 3.85 ppm) and in GPMS (2.52, 2.69, and 3.32 ppm), with respect to the number of protons of aromatic rings in DGEBA (6.87 and 7.21 ppm) and the α-CH_2 in GPMS (0.64 ppm). The only rather unexpected finding was the persistence of a small concentration of $-OCH_3$ protons of GPMS, at 3.53 ppm. In the silsesquioxane, they were partially superimposed to the peak of γ-CH_2 protons of GPMS, at 3.44 ppm. It was estimated that about 7% of the initial Si$-OCH_3$ groups were not hydrolyzed under the selected reaction conditions.

^{29}Si NMR spectra showed the presence of a broad peak in the region −64 to −72 ppm, with maxima at −66.66 and −68.15 ppm, assigned to Si atoms joined to three other Si atoms through Si−O−Si bonds, in unstrained structures.[4,14−18] A smaller peak in the region −54 to −62 ppm, with maxima at −58.8 and −60.3 ppm, was assigned to Si atoms bonded to three other Si atoms through Si−O−Si bonds, present in strained Si_3O_3 rings, and to Si atoms bonded to two other Si atoms through Si−O−Si bonds and to an OH group (or eventually a methoxy group).[4,19,20] Small peaks at −42.52 and −50.83 ppm were assigned to the monomer and dimer that are still present in the final products.[19,21]

FTIR spectra showed that a relatively low amount of SiOH groups still persisted as revealed by the presence of a small band at 3485 cm^{-1}.

^{1}H NMR, ^{29}Si NMR, and FTIR Characterization of the SSQO Based on MPMS. ^{1}H NMR spectra of the silsesquioxane represented by the SEC chromatogram of the product stored at 23 °C in Figure 6 showed that the 3-methacryloxypropyl residue remained intact. No protons assignable to Si$-OCH_3$, HCOOH, CH_3OH, or $HCOOCH_3$ were detected, meaning that the hydrolysis was complete and volatiles were eliminated. (Traces of the undeuterated solvent, Cl_3CH, appeared at 7.27 ppm.) A small band at 2.21 ppm was assigned to SiOH groups that do not exhibit H-bonds to other SiOH groups.[4,14−16,20] The fraction of protons associated with this peak was 0.16 SiOH/Si. This means that about 16% of the initial Si atoms are joined to hydroxy groups while the remaining 84% are fully condensed.

^{29}Si NMR spectra showed the presence of two broad peaks of about the same magnitude. The first one exhibited a sharp maximum at −58.069 ppm while the second one showed two maxima at −65.586 and −66.567 ppm. The former was assigned to Si atoms bonded to three other Si atoms through Si−O−Si bonds, present in strained Si_3O_3 rings, and to Si atoms bonded to two other Si atoms through Si−O−Si bonds and to an OH group.[4,19,20] The latter was assigned to Si atoms joined to three other Si atoms through Si−O−Si bonds, in unstrained structures.[4,14−18,22]

FTIR spectra showed a broad band with a maximum at 3482 cm^{-1}, ascribed to stretching of OH of SiOH groups that are hydrogen bonded to CO groups. (A shoulder at 1700 cm^{-1} on the CO band at 1720 cm^{-1} arises from CO that is hydrogen bonded to SiOH groups.[23]) The 2841 cm^{-1} band present in MPMS and assigned to the CH_3 symmetric stretch of the OCH_3 groups was absent in the silsesquioxane, in agreement with the absence of OCH_3 peaks in ^{1}H NMR spectra.

UV-MALDI-TOF MS of the Silsesquioxane Derived from MPMS. To understand the way in which larger clusters are formed, UV-MALDI-TOF MS spectra of the more condensed SSQO (SEC chromatogram in Figure 8) will be analyzed. As described in the Experimental Section, two different instruments, several matrices, and two preparation methods including doping solutions were used. Results will be illustrated with a series obtained with the MALDI III device operating in the positive ion mode, using GA as matrix, method B of sample preparation, and eventually using Na^+ or Ag^+ for doping purposes. In every case, the cations correspond to a particular species that added a Na^+. These results could be reproduced using different matrices, sample preparation methods, analyte/matrix ratios, laser powers, and operation modes.

Figure 9 shows the full mass spectrum of the more condensed SSQO derived from MPMS. Two major clusters are observed: the first one peaking at *m*/*z* 1284.3 and the second one at *m*/*z* 3653.0. But other significant peaks corresponding to larger species were reproducibly found under different experimental conditions, at *m*/*z* 6546.7 and 9420.4.

Figure 10 shows a magnification of the molar mass distribution of the first cluster. Assignment of peaks is shown in Table 1. Species are clearly identified taking into account a consistent shift of about 2 *m*/*z* unities with respect to the calibration. Most of the species are incompletely condensed polyhedra with 6−11 Si atoms (species with 12, 13, ... Si atoms are also present), with a very small fraction of perfect polyhedra (T_6 and T_8). Predominant species are $T_7(OH)$, $T_8(OH)_2$, and $T_9(OH)$. This agrees with SEC results that indicated that the first cluster was centered at about $n = 8$. The species $T_7(OH)$ located at the maximum of the distribution contains a Si_3O_3 strained ring. Feher et al.[4] could identify a similar species with R = cyclohexyl instead of 3-methacryloxypropyl, but they reported that it slowly decomposed on standing. The nature of the R group seems to be important for stabilizing this species. (In particular, the carbonyl of the 3-methacryloxypropyl can give an H bond with the OH group, as inferred from FTIR spectra.) The presence of $T_7(OH)$ as the main species in the first cluster was reconfirmed by adding AgTFA to the sample to have the possibility of detecting species charged with Ag^+. A new peak at *m*/*z* 1370.1 appeared that was assigned to $T_7(OH) + Ag^+$ (calculated mass = 1371.6).

Figure 11 shows a magnification of the molar mass distribution of the second cluster. Assignment of peaks is shown in Table 2. Every *n*-mer is represented in the series. For the smaller species two peaks are clearly distinguished in the major peak; e.g., both $T_{13}(OH)$ and $T_{13}(OH)_3$ are present. For the larger species a single peak is observed which, in some cases, is assigned to the sum of two species, as indicated in Table 2. Larger species that were clearly distinguished in every spectra were assigned to $T_{36}(OH)_8$ (calculated mass = 6525; experimental $m/z - Na^+ = 6524$) and $T_{52}(OH)_8$ (calculated mass = 9393; experimental $m/z - Na^+ = 9397$).

The fraction of SiOH groups varies from 0.11 to 0.25 for the main species of the first cluster and from 0.14

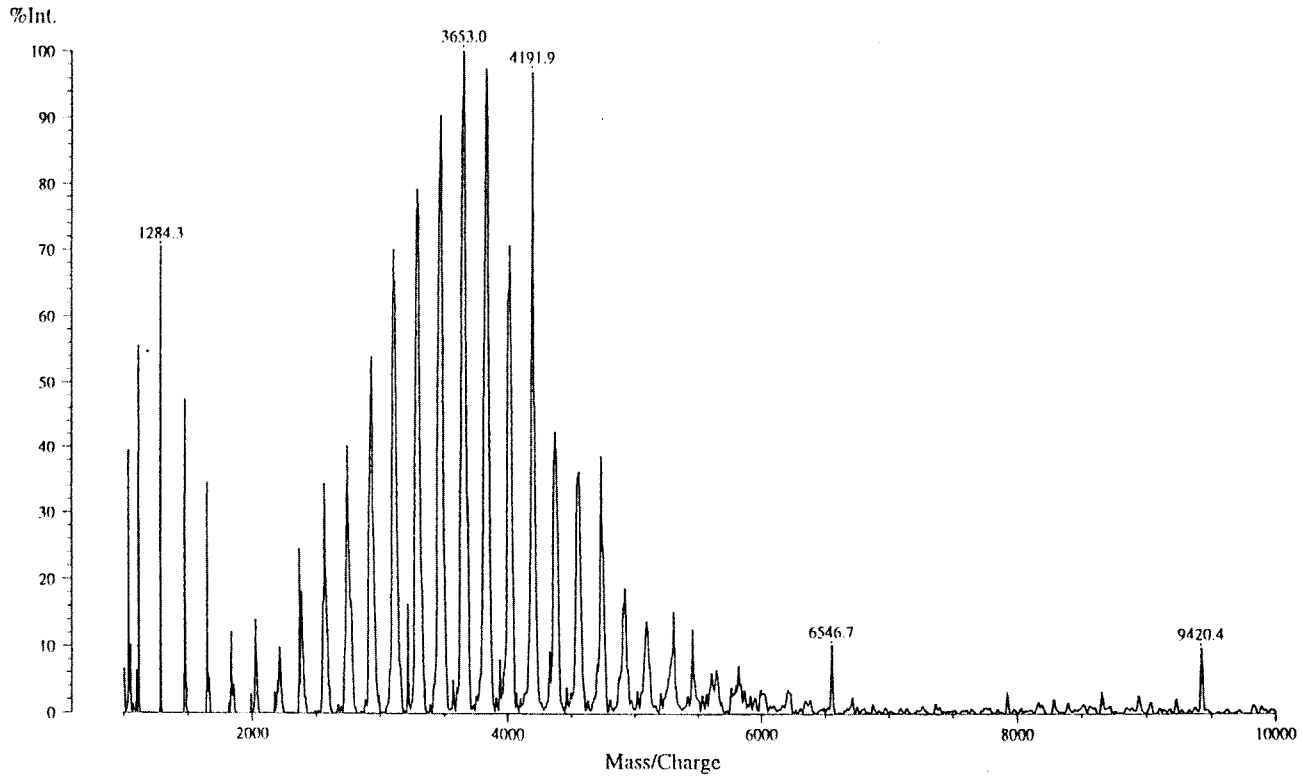

Figure 9. UV-MALDI-TOF mass spectrum of the more condensed SSQO derived from MPMS (positive mode; matrix GA; sample doped with NaCl).

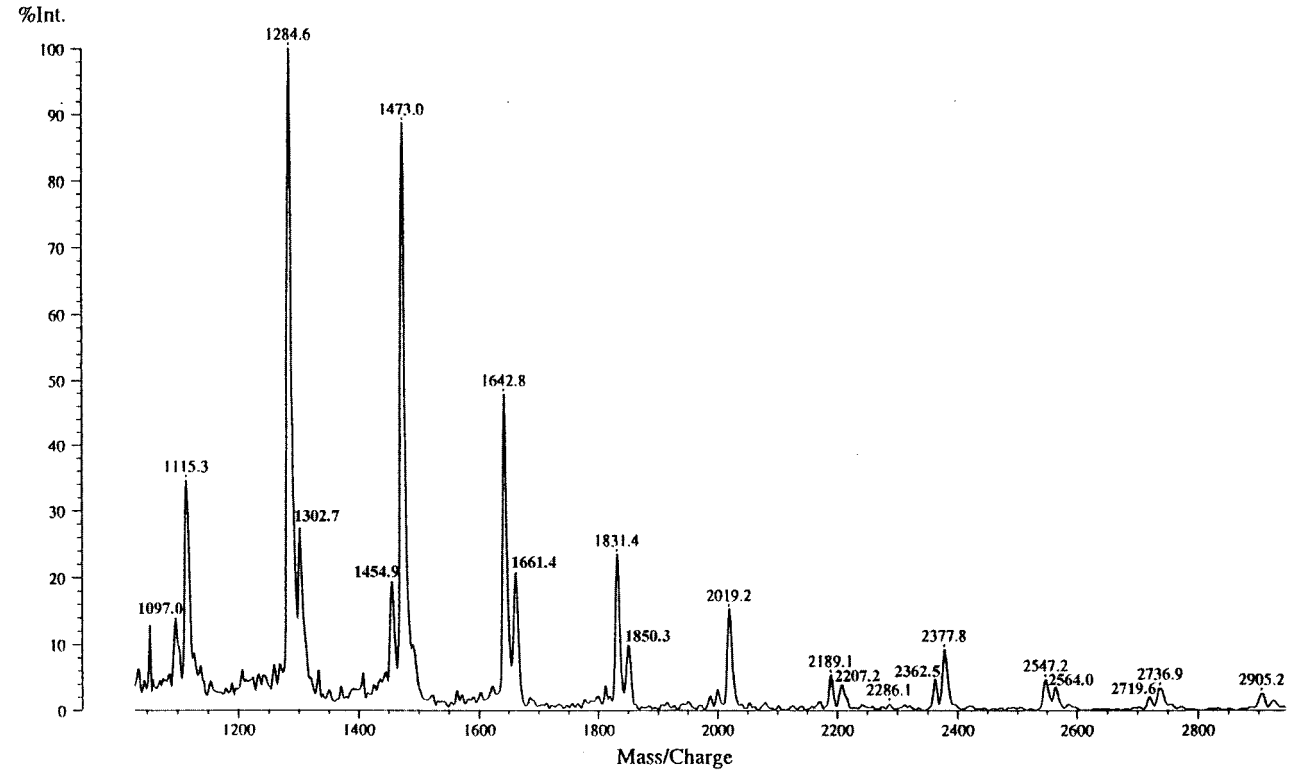

Figure 10. Partial UV-MALDI-TOF mass spectrum of the more condensed SSQO derived from MPMS (positive mode; matrix GA; *m*/*z* range 1100−2900).

to 0.30 for the main species of the second cluster. This compares relatively well with the experimental value of 0.16 found by ^{1}H NMR.

The way by which the silsesquioxane structure has been built up may be now analyzed. Major species remaining in the first cluster are plausibly the less reactive ones. One may speculate that the following particular species, with 2−4 OH groups per molecule, had significant concentrations at the time when the first cluster was formed: $T_7(OH)_3$, $T_8(OH)_2$, $T_9(OH)_3$, T_{10}-

Table 1. Assignment of UV-MALDI-TOF MS Peaks for Species of the First Cluster

exptl *m/z*	$m/z - Na^+$	assignt	calcd *m/z*
1097.0	1074.0	T_6	1075.5
1115.3	1092.3	$T_6(OH)_2$	1093.5
1284.6	1261.6	$T_7(OH)$	1263.7
1302.7	1279.7	$T_7(OH)_3$	1281.7
1454.9	1431.9	T_8	1434.0
1473.0	1450.0	$T_8(OH)_2$	1452.0
1642.8	1619.8	$T_9(OH)$	1622.2
1661.4	1638.4	$T_9(OH)_3$	1640.2
1831.4	1808.4	$T_{10}(OH)_2$	1810.5
1850.3	1827.3	$T_{10}(OH)_4$	1828.5
2019.2	1996.2	$T_{11}(OH)_3$	1998.7

Table 2. Assignment of UV-MALDI-TOF MS Peaks for Species of the Second Cluster

exptl *m/z*	$m/z - Na^+$	assignt	calcd *m/z*
2020.2	1997.2	$T_{11}(OH)_3$	1998.7
2208.7	2185.7	$T_{12}(OH)_4$	2187.0
2363.6	2340.6	$T_{13}(OH)$	2339.2
2562.8	2539.8	$T_{14}(OH)_2$, $T_{14}(OH)_4$	2527.5; 2545.5
2740.6	2717.6	$T_{15}(OH)_3$	2715.7
2928.6	2905.6	$T_{16}(OH)_4$	2904.0
3099.1	3076.1	$T_{17}(OH)_3$	3074.2
3284.4	3261.4	$T_{18}(OH)_4$	3262.5
3471.3	3448.3	$T_{19}(OH)_5$	3450.7
3653.0	3630.0	$T_{20}(OH)_4$, $T_{20}(OH)_6$	3621.0; 3639.0
3829.5	3806.5	$T_{21}(OH)_5$	3809.2
4014.1	3991.1	$T_{22}(OH)_4$, $T_{22}(OH)_6$	3979.4; 3997.4
4191.9	4168.9	$T_{23}(OH)_5$	4167.7
4371.4	4348.4	$T_{24}(OH)_4$, $T_{24}(OH)_6$	4337.9; 4355.9
4556.3	4533.3	$T_{25}(OH)_5$, $T_{25}(OH)_7$	4526.2; 4544.2
4732.0	4709.0	$T_{26}(OH)_4$, $T_{26}(OH)_6$	4696.4; 4714.4
4920.9	4897.9	$T_{27}(OH)_5$, $T_{27}(OH)_7$	4884.7; 4902.7
5090.5	5067.5	$T_{28}(OH)_4$, $T_{28}(OH)_6$	5054.9; 5072.9
5303.6	5280.6	$T_{29}(OH)_9$	5279.2
5451.1	5428.1	$T_{30}(OH)_6$	5431.4

$(OH)_4$, $T_{11}(OH)_3$, and $T_{12}(OH)_4$. These fundamental building blocks are incompletely condensed polyhedra or ladder structures.

Major species present in the second cluster were possibly formed by condensation of the major species of the first cluster. This explains the presence of every structure going from $T_{14}(OH)_4$ (formed by the condensation of two $T_7(OH)_3$) to $T_{24}(OH)_6$ (formed by the condensation of two $T_{12}(OH)_4$). The species $T_{24}(OH)_4$ may be formed by elimination of two molecules of water during the condensation of two $T_{12}(OH)_4$, or, alternatively, may be one of the structures formed in a third generation. Species belonging to the second cluster may be regarded as combinations of incompletely condensed polyhedra and ladder structures.

A third generation of structures is formed by condensation of species present in the first and second clusters. This accounts for the formation of the rest of species in Table 2 (including some of the structures belonging to the second generation), except those containing 7 or 9 OH groups per molecule. The latter may be formed by the reaction of more open structures that are present in minor amounts in the final distribution (e.g., $T_{29}(OH)_9$ may have been formed by condensation of $T_{22}(OH)_8$ with $T_7(OH)_3$).

The species $T_{36}(OH)_8$ may be generated through the condensation of $T_{12}(OH)_4$ with $T_{24}(OH)_6$ (or other possible combinations). The largest species that was detected in significant amounts was $T_{52}(OH)_8$. It may be formed in a fourth generation by different possible combinations (e.g., $T_{12}(OH)_4 + T_{20}(OH)_4 + T_{20}(OH)_4$). The presence of $T_{36}(OH)_8$ and $T_{52}(OH)_8$ in the final SSQO gives a hint of the presence of $T_8(OH)_2$ and $T_{12}(OH)_4$ as key species in the polymer growth (their reaction gives $T_{20}(OH)_4$).

UV-MALDI-TOF MS results confirmed the presence of a cluster-growth mechanism in the synthesis of the more condensed SSQO derived from MPMS. During the initial stage of the hydrolytic condensation, species with *n* values comprised in the range 7−12 are produced.

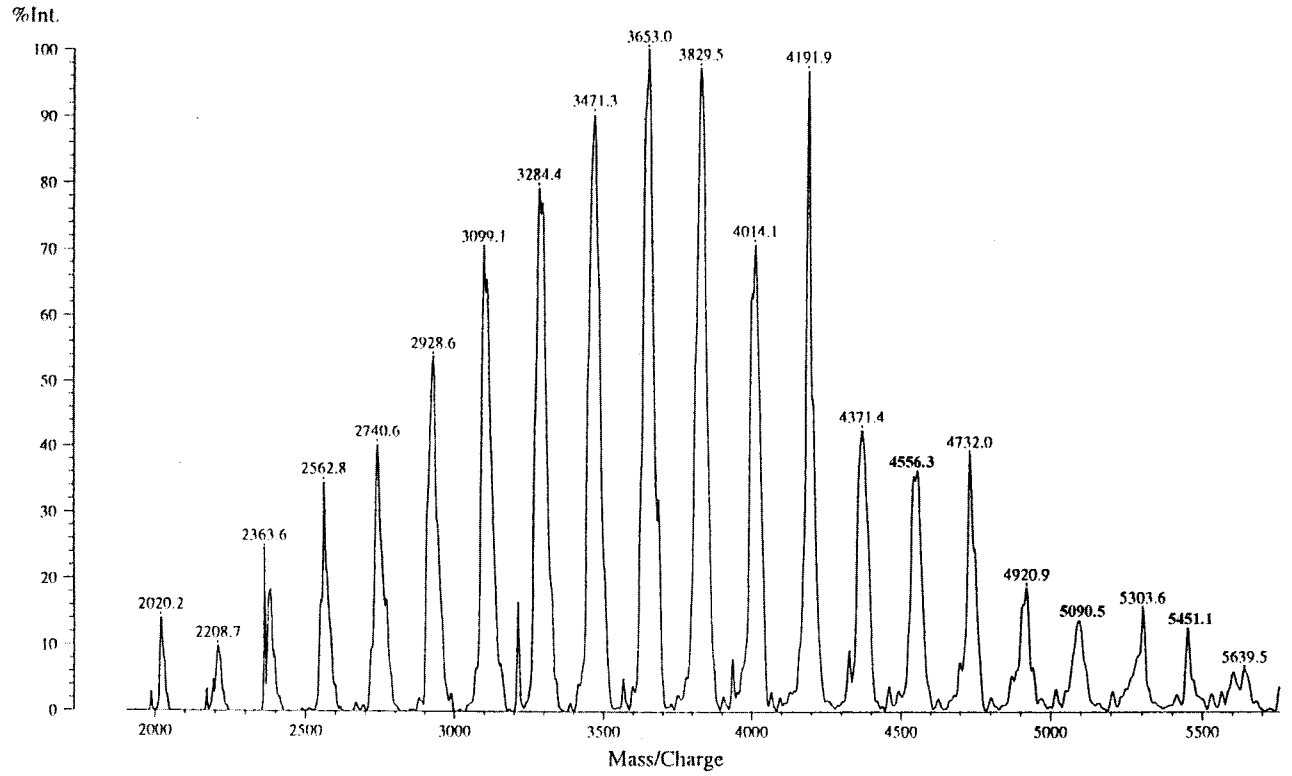

Figure 11. Partial UV-MALDI-TOF mass spectrum of the more condensed SSQO derived from MPMS (positive mode; matrix GA; sample doped with NaCl; *m/z* range 2000−5700).

They mainly consist of incompletely condensed polyhedra (species with 1−3 OH per molecule) and ladder-type structures (species with 4 OH per molecule). Species with more OH groups are condensed with a higher probability, giving place to a second generation of condensation products. This process accounts for the presence of the cluster with *n* values in the range 14−24 and the enrichment of the first cluster in the more condensed structures ($T_7(OH)$, $T_8(OH)_2$, and $T_9(OH)$). A third and fourth generation of condensation products are also present. Some species may be formed in a second or in a third generation. For example, this is the case of $T_{23}(OH)_5$ which may be formed in a second generation ($T_{11}(OH)_3 + T_{12}(OH)_4$) or in a third generation ($T_{16}(OH)_4 + T_7(OH)_3$). Its particular high concentration (see Figure 11) may be the result of the possibility of its formation in two different generations. Structures of different species may be depicted as combinations of incompletely condensed polyhedra with ladder fragments. An analysis of the mass distributions of SSQO derived from MPMS but showing different degrees of condensation will be the subject of a future publication.

Conclusions

(a) High-molar-mass silsesquioxanes polyfunctionalized with epoxy or methacrylic groups could be synthesized in a reactive solvent (DGEBA) and in bulk, respectively. The organic functional groups remained unreacted during the hydrolytic condensation process, as revealed by ^{1}H NMR.The resulting silsesquioxanes showed a very good stability and could be used to synthesize inorganic−organic hybrid materials by polymerizing the organic functional groups.[24,25]

(b) The silsesquioxane growth was followed by SEC for both starting silanes. Molar-mass distributions showed the presence of clusters corresponding to products formed in different generations. With the aid of UV-MALDI-TOF MS, the different species present in every cluster could be identified for one of the silsesquioxanes derived from MPMS. During the initial stage of the hydrolytic condensation, species with 7−12 Si atoms are produced. They mainly consist of incompletely condensed polyhedra (species with 1−3 OH per molecule) and ladder-type structures (species with 4 OH per molecule). Species with more OH groups are condesed with a higher probability, giving place to a second generation of condensation products. This process accounts for the presence of the cluster of species with 14−24 Si atoms and the enrichment of the first cluster in the more condensed structures ($T_7(OH)$, $T_8(OH)_2$, and $T_9(OH)$). A third and fourth generation of condensation products are also present. Structures of different species may be depicted as combinations of incompletely condensed polyhedra with ladder fragments.

Acknowledgment. We acknowledge the financial support of CONICET, ANPCyT, Universities of Buenos Aires and Mar del Plata and INTI, Argentina. R. Erra-Balsells, C. C. Riccardi, and R. J. J. Williams are Research Members of CONICET. UV-MALDI TOF MS experiments were performed as part of the Academic Agreement between Rosa Erra-Balsells and Hiroshi Nonami with the facilities of the High Resolution Liquid Chromatography-Integrated Mass Spectrometer System of the United Graduated School of Agricultural Sciences (Ehime University, Japan).

References and Notes

(1) Brown, Jr., J. F.; Vogt, Jr., L. H.; Prescott, P. I. *J. Am. Chem. Soc.* **1964**, *86*, 1120−1125.
(2) Brown, Jr., J. F.; Vogt, Jr., L. H. *J. Am. Chem. Soc.* **1965**, *87*, 4313−4317.
(3) Brown, Jr., J. F. *J. Am. Chem. Soc.* **1965**, *87*, 4317−4324.
(4) Feher, F. J.; Newman, D. A.; Walzer, J. F. *J. Am. Chem. Soc.* **1989**, *111*, 1741−1748.
(5) Baney, R. H.; Itoh, M.; Sakakibara, A.; Suzuki, T. *Chem. Rev.* **1995**, *95*, 1409−1430.
(6) Lichtenhan, J. D. *Comments Inorg. Chem.* **1995**, *17*, 115−130.
(7) Piana, K.; Schubert, U. *Chem. Mater.* **1994**, *6*, 1504−1508.
(8) Wallace, W. E.; Guttman, C. M.; Antonucci, J. M. *J. Am. Soc. Mass Spectrom.* **1999**, *10*, 224−230.
(9) Antonucci, J. M.; Fowler, B. O.; Stansbury, J. W. *ACS Polym. Prepr.* **1997**, *38*, 118−119.
(10) Sharp, K. *J. Sol-Gel Sci. Technol.* **1994**, *2*, 35−41.
(11) Nonami, H.; Fukui, S.; Erra-Balsells, R. *J. Mass Spectrom.* **1997**, *32*, 287−296.
(12) Nonami, H.; Tanaka, K.; Fukuyama, Y.; Erra-Balsells, R. *Rapid Commun. Mass Spectrom.* **1998**, *12*, 285−296.
(13) Belu, A. M.; DeSimone, J. M.; Linton, R. W.; Lange, G. W.; Friedman, R. M. *J. Am. Soc. Mass Spectrom.* **1996**, *7*, 11−24.
(14) Feher, F. J.; Budzichowski, T. A.; Blanski, R. L.; Weller, K. J.; Ziller, J. W. *Organometallics* **1991**, *10*, 2526−2528.
(15) Feher, F. J.; Soulivong, D.; Eklund, A. G. *Chem. Commun.* **1998**, 399−400.
(16) Feher, F. J.; Soulivong, D.; Nguyen, F. *Chem. Commun.* **1998**, 1279−1280.
(17) Feher, F. J.; Wyndham, K. D.; Soulivong, D.; Nguyen, F. *J. Chem. Soc., Dalton Trans.* **1999**, 1491−1497.
(18) Feher, F. J.; Budzichowski, T. A. *J. Organomet. Chem.* **1989**, *373*, 153−163.
(19) Unno, M.; Alias, S. B.; Saito, H.; Matsumoto, H. *Organometallics* **1996**, *15*, 2413−2414.
(20) Feher, F. J.; Soulivong, D.; Lewis, G. T. *J. Am. Chem. Soc.* **1997**, *119*, 11323−11324.
(21) Besland, M. P.; Guizard, C.; Hovnanian, N.; Larbot, A.; Cot, L.; Sanz, J.; Sobrados, I.; Gregorkiewitz, M. *J. Am. Chem. Soc.* **1991**, *113*, 1982−1987.
(22) Lichtenhan, J. D.; Otonari, Y. A.; Carr, M. J. *Macromolecules* **1995**, *28*, 8435−8437.
(23) Ishida, H.; Naviro, S.; Koenig, J. L. *Physicochemical Aspects of Polymer Surfaces*; Plenum: New York, 1983; Vol. 1, p 91.
(24) Eisenberg, P.; Lucas, J. C.; Williams, R. J. J. *Polimery* **1999**, *44*, 735−739.
(25) Mauri, A. N.; Riccardi, C. C.; Williams, R. J. J. *Macromol. Symp.*, in press.

MA9912507